Thermal modeling and identification of an aluminum rod using fractional calculus

Rachid R. Malti, Jocelyn Sabatier, Hüseyin Akçay

Thermal modeling and identification of an aluminum rod using fractional calculus

Rachid Malti, * **Jocelyn Sabatier,** * **and Hüseyin Akçay** **

* *Université de Bordeaux, IMS, UMR 5218 CNRS, 351 cours de la Libération, 33405 Talence cedex, France*
{*rachid.malti, jocelyn.sabatier*}*@laps.ims-bordeaux.fr*
** *Center for Systems Engineering and Applied Mechanics (CESAME), Université Catholique de Louvain, B-1348 Louvain-la-Neuve, Belgium*

Abstract: the aim of this paper is to model thermal flux versus temperature in an aluminum rod. The objective is to check whether a theoretical model applies to experimental data and then to investigate some more effective fractional models from black box identification. For this particular system, it is shown that fractional models are more suitable than rational ones, since they require fewer parameters to achieve the same quality of approximation.

Keywords: continuous-time models; fractional calculus; system identification; output error.

1. INTRODUCTION

Fractional calculus is a generalization of the traditional calculus and dates back to Liouville [1832] and Riemann [1892]. It remained for a long time an interesting but abstract mathematical concept. The past two decades have witnessed considerable development in the use of fractional calculus in various fields. It is now an important tool for the international scientific and industrial communities.

Many diffusive phenomena can be modeled by fractional transfer functions. In electrochemistry for instance, diffusion of charges in acid batteries is governed by Randles models (Rodrigues et al. [2000], Sabatier et al. [2006]) that involve Warburg impedance with an integrator of order 0.5. Electrochemical diffusion, investigated in semi-infinite planar, spherical and cylindrical media by Oldham and Spanier [1970, 1972, 1973], showed to have a tight relation with derivatives of order 0.5. In thermal diffusion of a semi-infinite homogeneous medium, Battaglia et al. [2001] have shown that the exact solution for the heat equation links thermal flux to a half order derivative of the surface temperature on which the flux is applied.

The objective here is to investigate thermal diffusion in an aluminum rod and to check whether the theoretical model of thermal diffusion applies to experimental data. Then, a more effective fractional model is determined using black box identification and compared to rational models obtained in the same manner.

The paper is organized as follows. After a mathematical background on fractional derivatives, a physical model of the aluminum rod is elaborated under some simplifying assumptions. Then, in section 3, the system is identified in a black box context and the obtained fractional models are compared to rational models identified using the ContSid toolbox Garnier et al. [2006].

1.1 Mathematical background

A fractional mathematical model is based on a fractional differential equation:

$$y(t) + a_1 \mathbf{D}^{\alpha_1} y(t) + \cdots + a_{m_A} \mathbf{D}^{\alpha_{m_A}} y(t) = b_0 \mathbf{D}^{\beta_0} u(t) + b_1 \mathbf{D}^{\beta_1} u(t) + \cdots + b_{m_B} \mathbf{D}^{\beta_{m_B}} u(t) \quad (1)$$

where $(a_j, b_i) \in \mathbb{R}^2$, differentiation orders

$$\alpha_1 < \alpha_2 < \ldots < \alpha_{m_A}, \quad (2)$$

$$\beta_0 < \beta_1 < \ldots < \beta_{m_B}. \quad (3)$$

are allowed to be non-integer positive numbers. The concept of differentiation to an arbitrary (non-integer) order γ, with $\gamma \in \mathbb{R}_+^*$ (set of strictly positive real numbers):

$$\mathbf{D}^{\gamma} \triangleq \left(\frac{d}{dt}\right)^{\gamma}, \quad (4)$$

was defined in the 19$^{\text{th}}$ century by Riemann and Liouville. The γ-order fractional derivative of $x(t)$ is defined as being an integer derivative of order $\lfloor\gamma\rfloor + 1$ ($\lfloor.\rfloor$ stands for the floor operator) of a non-integer integral of order $\lfloor\gamma\rfloor - \gamma + 1$ Samko et al. [1993]:

$$\mathbf{D}^{\gamma} x(t) = \mathbf{D}^{\lfloor\gamma\rfloor+1} \left(\mathbf{I}^{\lfloor\gamma\rfloor+1-\gamma} x(t)\right) \triangleq \left(\frac{d}{dt}\right)^{\lfloor\gamma\rfloor+1} \left(\frac{1}{\Gamma\left(\lfloor\gamma\rfloor + 1 - \gamma\right)} \int_0^t \frac{x(\tau)\, d\tau}{(t-\tau)^{\gamma-\lfloor\gamma\rfloor}}\right), \quad (5)$$

where $t > 0$, $\gamma \in \mathbb{R}_+^*$, and the Euler's Γ function is defined in the set of real numbers except zero and negative integers ($x \in \mathbb{R}^* \setminus \mathbb{N}^-$) as:

$$\Gamma(x) = \int_0^{\infty} e^{-t} t^{x-1} dt. \quad (6)$$

The Laplace transform is a more concise algebraic tool generally used to represent fractional systems Oldham and Spanier [1974]:

$$\mathscr{L}\left\{\mathbf{D}^{\gamma} x(t)\right\} = s^{\gamma} X(s) \quad \text{if } x(t) = 0 \ \forall t \leq 0. \quad (7)$$

This property allows to write the fractional differential equation (1), provided $u(t)$ and $y(t)$ equal 0 for all $t < 0$, in a transfer function form:

$$F(s) = \frac{B(s)}{A(s)} = \frac{\sum_{i=0}^{m_B} b_i s^{\beta_i}}{1 + \sum_{j=1}^{m_A} a_j s^{\alpha_j}}. \quad (8)$$

Moreover if $F(s)$ is commensurable of order γ, i.e. all differentiation orders are exactly divisible by the same number γ an integral number of times (the biggest number is always chosen), then $F(s)$ can be rewritten as:

$$F(s) = \frac{\sum_{i=0}^{n} \tilde{b}_i s^{i\gamma}}{1 + \sum_{j=1}^{m} \tilde{a}_j s^{j\gamma}}, \quad (9)$$

where $n = \frac{\beta_{m_B}}{\gamma}$ and $m = \frac{\alpha_{m_A}}{\gamma}$ are integers and:

$$\begin{cases} \tilde{b}_i = b_i \text{ if } i\gamma = \beta_i & \text{and } \tilde{b}_i = 0 \text{ if } i\gamma \neq \beta_i \\ \tilde{a}_j = a_j \text{ if } j\gamma = \alpha_j & \text{and } \tilde{a}_j = 0 \text{ if } j\gamma \neq \alpha_j. \end{cases} \quad (10)$$

In rational transfer functions γ equals 1 and usually numerator α_{m_A} and denominator β_{m_B} orders are both fixed, then all coefficients $b_i, i = 1, \ldots, \beta_{m_B}$ and $a_j, j = 1, \ldots, \alpha_{m_A}$ are estimated. Generally, no care is taken to check whether any intermediate coefficient, as in (10), equals zero.

1.2 Time-domain simulation of fractional models

Many different algorithms for simulating fractional systems in the time-domain exist (Aoun et al. [2004]). Although identification algorithms presented in our paper could be implemented with any of these simulation algorithms, the simulation algorithm used in our paper is explained here.

Due to the consideration that real physical systems generally have bandlimited fractional behavior and due to the practical limitations of input and output signals (Shannon's cut-off frequency for the upper band and the spectrum of the input signal for the lower band), fractional operators are usually approximated by high order rational models. As a result, a fractional model and its rational approximation have the same dynamics within a limited frequency band. The most commonly used approximation of s^ν, and by the way the one used in this paper, in the frequency band $[\omega_A, \omega_B]$ is the recursive distribution of zeros and poles proposed by Oustaloup [1995]:

$$s^\gamma \rightarrow s^\gamma_{[\omega_A,\omega_B]} = C_0 \left(\frac{1 + \frac{s}{\omega_A}}{1 + \frac{s}{\omega_B}} \right)^\gamma \approx C_0 \prod_{k=1}^{N} \frac{1 + \frac{s}{\omega'_k}}{1 + \frac{s}{\omega_k}}, \quad (11)$$

where $\omega_i = \alpha\omega'_i, \quad \omega'_{i+1} = \eta\omega'_i \quad$ and

$$\gamma = 1 - \frac{\log \alpha}{\log \alpha\eta}, \quad (12)$$

α and η define the differentiation order γ. The bigger N the better the approximation of the differentiator s^ν within $[\omega_A, \omega_B]$.

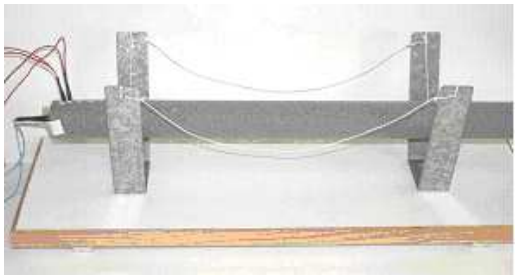

Fig. 1. Insulated long aluminum rod heated by a resistor

2. PHYSICAL MODELING OF THE ALUMINUM ROD

2.1 Plant description

A long aluminum rod heated by a resistor is considered in this experiment. To ensure unidirectional heat transfer, the entire surface of the rod is insulated by a foam as shown in Fig. 1. The input signal is a thermal flux generated by a resistor glued at one end and the output signal is the temperature of the rod measured at a distance x from the heated end.

The injected heat flux is controlled by a computer through an on-off transistor with a controlled amplitude of the input voltage. Temperature is measured using a platinum probe and an amplifier with a quantification error of 0.125 degree and which dynamic behavior is neglected.

2.2 Physical modeling

To demonstrate the fractional behavior of this thermal system, the aluminum rod is modeled under the following assumptions:

(i) the rod is perfectly isolated,
(ii) the rod is considered as a semi-infinite homogeneous plane medium with conductivity λ and diffusivity α,
(iii) at rest, the rod is at ambient temperature, so that there is no thermal exchange with the environment,
(iv) Losses on the surface where the thermal flux is applied are neglected. The electrical energy consumed in the resistor is assumed to be totally transformed into thermal energy and diffused by conduction in the only direction of the aluminum rod.

The last assumption is required in order to compute the thermal flux from the electrical energy injected in the resistor. Care is taken so that assumption (iii) is fulfilled. A time period of 24 hours is observed between two consecutive experiments so that the temperature of the aluminum rod cools down to the ambient temperature and hence initial conditions are zero at the beginning of each experiment, since there is initially no thermal exchange with the environment. Fractional systems with non zero initial conditions are much harder to tackle ; see Lorenzo and Hartley [2008], Sabatier et al. [2008].

A one-dimensional heat transfer is governed by the following partial differential equation and boundary effects:

$$\begin{cases} \dfrac{\partial T(x,t)}{\partial t} = \alpha \dfrac{\partial^2 T(x,t)}{\partial x^2}, 0 < x < \infty, t > 0 \\ -\lambda \dfrac{\partial T(x,t)}{\partial x} = \varphi(t), \qquad x = 0, \quad t > 0 \\ T(x,t) = 0, \qquad 0 \le x < \infty, \quad t = 0 \end{cases} \tag{13}$$

where $T(x,t)$ is the temperature measured at a distance x, φ is the injected heat flux, λ the thermal conductivity, and α the thermal diffusivity.

Evaluating the Laplace transform of the first equation leads to the ordinary differential equation:

$$\frac{\partial^2 \bar{T}(x,s)}{\partial x^2} - \frac{s}{\alpha}\bar{T}(x,s) = 0, \tag{14}$$

$$\text{where } \bar{T}(x,s) = \mathscr{L}\{T(x,t)\}. \tag{15}$$

Solving with respect to x yields:

$$\bar{T}(x,s) = K_1(s)\, e^{-x\sqrt{\frac{s}{\alpha}}} + K_2(s)\, e^{x\sqrt{\frac{s}{\alpha}}}. \tag{16}$$

Taking into account limit conditions, the following transfer function is obtained:

$$H(x,s) = \frac{\bar{T}(x,s)}{\bar{\varphi}(s)} = \frac{\sqrt{\alpha}}{\lambda\sqrt{s}}\, \mathrm{e}^{-x\sqrt{\frac{s}{\alpha}}}. \tag{17}$$

$\bar{\varphi}$ stands for the Laplace transform of φ.

Setting $z = x\sqrt{\frac{s}{\alpha}}$, and evaluating the P^{th} order Padé approximation of e^{-z} yields:

$$e^{-z} \approx \frac{\sum_{k=0}^{P} \frac{(2P-k)!}{k!(P-k)!}(-z)^k}{\sum_{k=0}^{P} \frac{(2P-k)!}{k!(P-k)!} z^k}. \tag{18}$$

Evaluating $H(x,s)$, at a fixed coordinate $x = x^*$, gives:

$$H(x^*,s) \approx H_P(s) = \frac{\sqrt{\alpha}}{\lambda\sqrt{s}} \frac{\sum_{k=0}^{P} \frac{(2P-k)!}{k!(P-k)!}(-x^*\sqrt{\frac{s}{\alpha}})^k}{\sum_{k=0}^{P} \frac{(2P-k)!}{k!(P-k)!}(x^*\sqrt{\frac{s}{\alpha}})^k}. \tag{19}$$

In the notation $H_P(s)$, the subscript P stands for the Padé approximation order. Note that $H_0(s)$ reduces to a simple integrator of order 0.5: $H_0(s) = \frac{\sqrt{\alpha}}{\lambda\sqrt{s}}$.

Values of physical parameters The following values of physical parameters are considered:

- the aluminum rod has a cylindrical shape with a length of 40cm and a diameter of 2cm,
- temperature (output signal) is measured at a distance $x^* = 0.5$cm, with a sampling period $T_s = 0.5$s.
- thermal conductivity and diffusivity of the aluminum rod are respectively: $\lambda = 237\ Wm^{-1}K^{-1}$ and $\alpha = 9975 \times 10^{-8}\ m^2/s$.

The integrator $H_0(s)$ and a first order order Padé approximation are respectively given by:

$$H_0(s) = \frac{4.21 \times 10^{-5}}{s^{0.5}}, \tag{20}$$

$$H_1(s) = \frac{10^{-5}}{s^{0.5}} \left(\frac{-2.11 s^{0.5} + 8.43}{0.50 s^{0.5} + 2.00} \right). \tag{21}$$

In Fig.2, the frequency response of the theoretical model (17) is compared to the integrator (20) and the first order

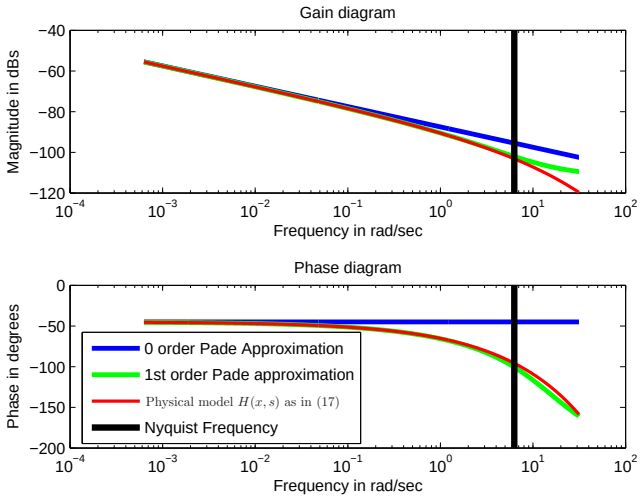

Fig. 2. Physical model $H(x,s)$ as in (17), and its Padé approximations $H_0(s)$ corresponding to a simple integrator and $H_1(s)$ as in (21).

Padé approximation (21) in a frequency band $[10^{-3}\ \ \omega_{Nq}]$, with ω_{Nq} Nyquist frequency. The first order Padé approximation matches quite well the theoretical model. Higher order Padé approximations are clearly unnecessary for a good approximation of the theoretical model up to the Nyquist frequency.

2.3 Applying experimental data to the physical model

The injected thermal flux is a pseudo random binary sequence (PRBS) varying from 0 to $\phi \approx 41\mathrm{KW/m^2}$. The injected heat flux is applied to the approximations $H_0(s)$ and $H_1(s)$ of the physical model $H(x,s)$ and the output of each model is compared to the measured temperature in Fig.3. The models exhibit similar dynamics as the true

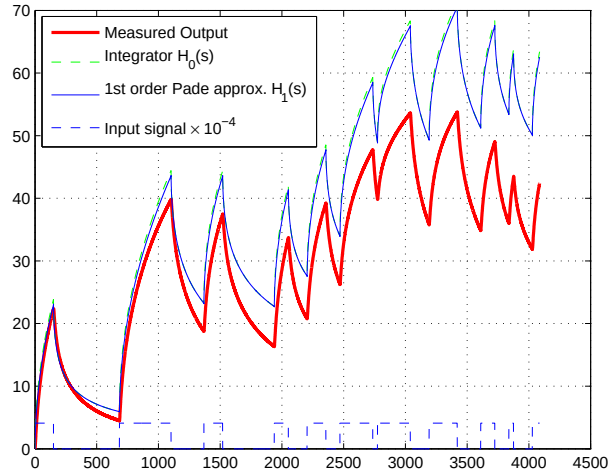

Fig. 3. Input/output experimental data and $H_0(s)$ and $H_1(s)$ model outputs.

system. However, system temperature increases less than model temperature which is most probably due to the heat

leakage. Assumption (i) p.2 is most probably violated as the aluminum rod is not perfectly isolated. Because of the heat leakage, hypothesis (ii) is violated either as the exact geometry (cylindrical) of the aluminum rod must be taken into account when considering boundary conditions.

All in all, the dynamical behaviors of the theoretical models might have been satisfactory, if the assumptions were satisfied. Unfortunately, this is not the case. So let's examine now the models obtained from a black box identification.

3. SYSTEM IDENTIFICATION IN AN OUTPUT ERROR CONTEXT

System identification using fractional models was initiated by Mathieu et al. [1995], Le Lay [1998], Cois et al. [2000, 2001]. Output-error-based methods (OE) applied on fractional models allow simultaneous estimation of differentiation orders and model parameters by Non Linear Programming (NLP) Malti et al. [2006].

OE methods for fractional models were first developed in Cois et al. [2000] who have chosen to represent the system in a modal form. They however constrained all s^γ-poles to be real-valued and of multiplicity one. In general, s^γ-poles can be real or complex conjugate, and of multiplicity greater or equal than one.

3.1 The OE model

The system to be identified is assumed to be initially at rest, modeled by (8) and characterized by input/output vector formed of coefficients and differentiation orders $\theta = [a_1, \dots a_{m_A}, b_0, \dots b_{m_B}, \alpha_1, \dots \alpha_{m_A}, \beta_0, \dots \beta_{m_B}]$. Constraints (2) and (3) are necessary for identifiability purposes.

When the number of parameters in (8) is high, optimization algorithms might be ill-conditioned. One way for limiting the number of parameters consists of optimizing the commensurable order γ instead of all differentiation orders. In this case, the fractional transfer function (8) is rewritten in a commensurable form as in (9). Numerator and denominator orders, respectively α_{m_A} and β_{m_B}, both multiples of γ, are fixed as in classical rational models. Henceforth, the system is entirely characterized by coefficients vector: $\theta = [\tilde{a}_1, \dots, \tilde{a}_{m_A}, \tilde{b}_0, \dots, \tilde{b}_{m_B}, \gamma]$. As far as identification of stable systems is concerned, the commensurable order is constrained to $]0, 2[$; see Matignon [1998] for details on stability of commensurable fractional systems.

Considering observed data $u(t)$ and $y^*(t) = y(t) + p(t)$, $p(t)$ being an output white noise, regularly sampled with a sampling period of T_s, the quadratic norm:

$$J\left(\hat{\theta}\right) = \sum_{k=0}^{K-1} \varepsilon^2\left(kT_s, \hat{\theta}\right) \tag{22}$$

of the output error:

$$\varepsilon\left(kT_s, \hat{\theta}\right) = y^*\left(kT_s\right) - \hat{y}\left(kT_s, \hat{\theta}\right) \tag{23}$$

is minimized. Model's output $\hat{y}(kT_s, \hat{\theta})$ being non linear in $\hat{\theta}$, gradient-based algorithms, such as the Marquardt algorithm (Marquardt [1963]), are used to estimate $\hat{\theta}$ iteratively:

$$\hat{\theta}_{i+1} = \hat{\theta}_i - \left\{\left[\mathbf{J}''_{\theta\theta} + \xi\mathbf{I}\right]^{-1}\mathbf{J}'_\theta\right\}_{\theta=\hat{\theta}_i}, \tag{24}$$

$$\begin{cases} \mathbf{J}'_\theta = -2\sum_{k=0}^{K-1} \varepsilon\left(kT_s\right)\mathbf{S}\left(kT_s, \hat{\theta}\right): \text{gradient} \\ \mathbf{J}''_{\theta\theta} \approx 2\sum_{k=0}^{K-1} \mathbf{S}\left(kT_s, \hat{\theta}\right)\mathbf{S}^{\mathrm{T}}\left(kT_s, \hat{\theta}\right): \text{pseudo} - \text{Hessian} \\ \mathbf{S}\left(kT_s, \hat{\theta}\right) = \dfrac{\partial\hat{y}\left(kT_s, \hat{\theta}\right)}{\partial\theta}: \text{output sensitivity functions} \\ \xi \ : \quad \text{Marquardt parameter} \end{cases} \tag{25}$$

Output sensitivity functions can be computed by differentiating (9) with respect to $\tilde{b}_i$, $\tilde{a}_k$ and γ (see Malti et al. [2006] for details).

3.2 Application to the aluminum rod under study

The OE model is now used for the identification of the aluminum rode based on measurement data. A two stage algorithm is applied. First of all, a model is estimated with an optimal commensurable order (reduced number of parameters) which is then used as an initial guess to compute an optimal model with all differentiation orders optimized.

Based on the study of the physical model, the following model structures are chosen:

$$\tilde{H}_0(s) = \frac{b_0}{s^{\alpha_0}}, \tag{26}$$

$$\tilde{H}_1(s) = \frac{b_0}{s^{\alpha_0}(a_1 s^{\alpha_1} + 1)}, \tag{27}$$

and their optimal parameters estimated.

A time lag of three samples (1.5 sec) is noticed between the input and the output signals, probably due to the time-lag in flux diffusion in the medium. Consequently, the following optimal models are obtained

$$\tilde{H}_0(s) = \frac{4.8 \times 10^{-5}}{s^{0.45}} \times e^{-1.5s}, \tag{28}$$

$$\tilde{H}_1(s) = \frac{19 \times 10^{-5}}{s^{0.29}(16s^{0.59} + 1)} \times e^{-1.5s}. \tag{29}$$

System and models outputs are plotted in Fig.4 on identification data and in Fig.5 on validation data. The model $\tilde{H}_1(s)$ clearly exhibits a better performance. Moreover, the normalized mean squared error is computed (with $x = id$ for identification data and $x = val$ for validation data):

$$J_x = \frac{J(\hat{\theta})}{\sum_{k=0}^{K-1}\left(y^*(kT_s)\right)^2}. \tag{30}$$

The performance index J_x is given for every model in the first two lines of Table 1.

It is interesting to notice, in validation data, that the model $\tilde{H}_1(s)$ fits exactly the measured output up to $t \approx 2500$s, and then there is a deviation between these two

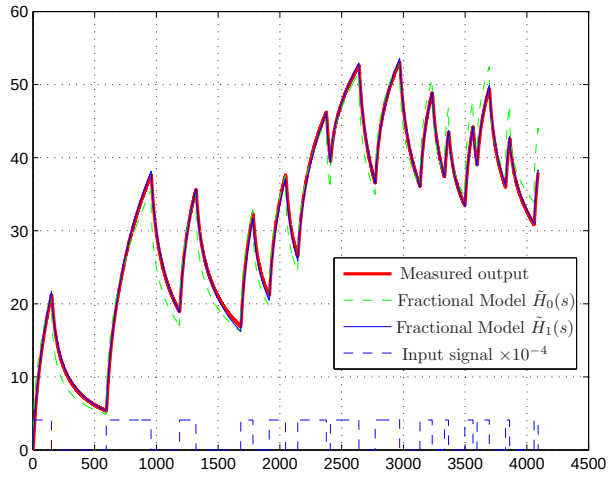

Fig. 4. Measured output compared to fractional models outputs on identification data

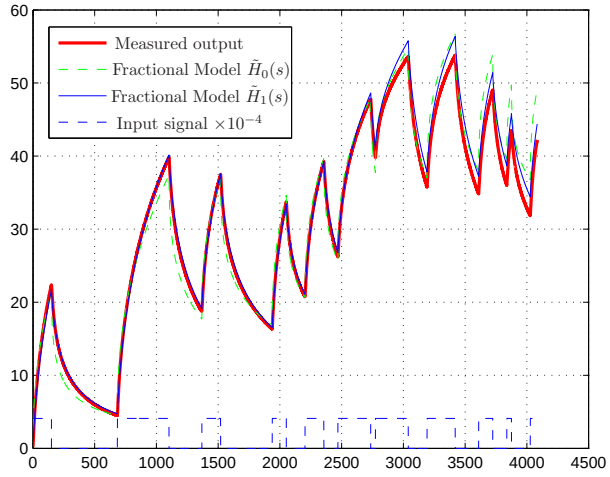

Fig. 5. Measured output compared to fractional models outputs on validation data

signals. This is most probably due to the presence of a fractional integrator in the model. Like integer integrators, fractional integrators accumulate the output signal. The difficulty with fractional integrators is that there exact value is unknown and even if it is approximated with a good precision, during long-time experiments, model integrator might accumulate the signal in a different way as compared to the true system integrator. In the frequency domain, long-time behavior is reflected in low frequencies. Hence in the presence of a fractional integrator, the slope of Bode's gain diagram is non zero in low frequencies as in Fig. 7. The difficulty with fractional integrators is that there exact slope is unknown and even if it is approximated with a good precision, below the spectrum of input/output data (below 6×10^{-3} in Fig. 7), model integrator might be different from true system integrator which again explains the time-domain deviation after $t \approx 2500$s.

Model	numb. of opt. param.	J_{id}	J_{val}
Fractional model $\tilde{H}_0$	2	4.24‰	5.30‰
Fractional model $\tilde{H}_1$	4	0.11‰	1.65‰
Rational model F_2	4	5.06‰	6.11‰
Rational model F_4	8	0.01‰	1.39‰

Table 1. Comparison between fractional and rational models.

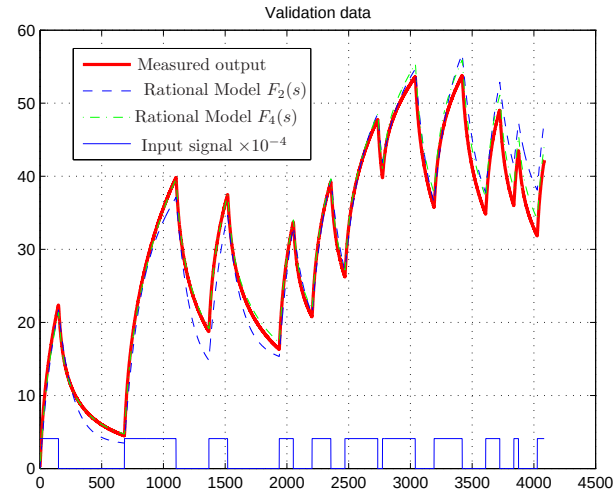

Fig. 6. Measured output compared to rational models outputs on validation data

3.3 Comparison with continuous-time rational models

Continuous-time rational OE model is used for the identification of the aluminum rode based on measurement data. For a fair comparison, a second order model $F_2(s)$ is first computed with the same number of parameters (four) as the fractional model $\tilde{H}_1(s)$. The `coe` function of the ContSid toolbox (Garnier et al. [2006]) is used and the following model obtained:

$$F_2(s) = \frac{5.86 \times 10^{-6}(s + 10^{-3})}{s^2 + 8.8 \times 10^{-3} s + 1.25 \times 10^{-6}} \times e^{-1.5s}. \quad (31)$$

Then, model order is augmented until the performance of the new rational model becomes comparable to the fractional one on the basis of identification and validation criteria. The fourth order model $F_4(s)$ as in (32) is obtained.

The performance index J_x of every rational model is given in the last two lines of Table 1. If one focuses on the validation index (J_{val} column), then he or she can verify that for a rational model eight parameters are required to reach a comparable validation index as a four-parameters fractional model.

This example clearly shows that fractional models are more adapted than rational models in modeling temperature versus heat flux in an aluminum rod, since they require less parameters. As explained in section 1.2 it is always possible to find a high order rational model equivalent to a fractional one in a given frequency band. High order rational models are necessary to get comparable results.

$$F_4(s) = \frac{1.17 \times 10^{-6} s^3 + 6.09 \times 10^{-6} s^2 + 1.17 \times 10^{-7} s + 1.97 \times 10^{-10}}{s^4 + 0.76 s^3 + 0.03 s^2 + 0.00017 s + 8.451 \times 10^{-08}} \times e^{-1.5s}. \quad (32)$$

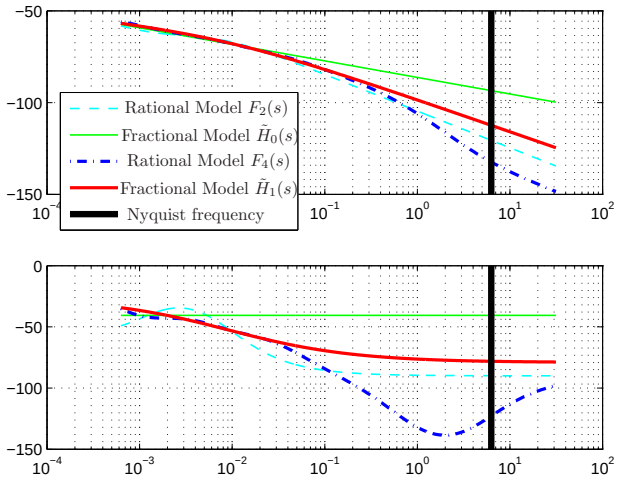

Fig. 7. Measured output compared to rational models outputs on identification data

4. CONCLUSIONS

Heat transfer in an aluminum rod was studied in this paper using real experimental data. It was shown that fractional models are more adapted for modeling this system since they require much less parameters to achieve a good quality of identification as compared to rational models. Higher order rational models are necessary to achieve comparable results.

REFERENCES

M. Aoun, R. Malti, F. Levron, and A. Oustaloup. Numerical simulations of fractional systems: an overview of existing methods and improvements. *An Int. J. of Nonlinear Dynamics and Chaos in Engineering Systems. Special issue: Fractional Derivatives and Their Applications*, 38(1-4):117–131, December 2004.

J.-L. Battaglia, O. Cois, L. Puigsegur, and A. Oustaloup. Solving an inverse heat conduction problem using a non-integer identified model. *Int. J. of Heat and Mass Transfer*, 44(14):2671–2680, 2001.

O. Cois, A. Oustaloup, E. Battaglia, and J.-L. Battaglia. Non integer model from modal decomposition for time domain system identification. In *proceedings of 12th IFAC Symposium on System Identification, SYSID*, Santa Barbara, USA, June 2000.

O. Cois, A. Oustaloup, T. Poinot, and J.-L. Battaglia. Fractional state variable filter for system identification by fractional model. In *IEEE 6th European Control Conference (ECC'2001)*, Porto, Portugal, Sep. 2001.

H. Garnier, M. Gilson, and O. Cervellin. Latest developments for the matlab contsid toolbox. *SYSID*, 2006. Newcastle, Australia.

L. Le Lay. *Identification fréquentielle et temporelle par modèle non entier*. PhD thesis, Université Bordeaux 1, Talence, France, 1998.

J. Liouville. Mémoire sur quelques questions de géométrie et de mécanique et sur un nouveau genre de calcul pour résoudre ces équations. *École polytechnique*, 13:71–162, 1832.

C.F. Lorenzo and T.T. Hartley. Initialization of fractional-order operators and fractional differential equations. *Journal of computational and nonlinear dynamics. Special issue on discontinuous and fractional dynamical systems*, 3:021101–1, 021101–9, April 2008.

R. Malti, M. Aoun, J. Sabatier, and A. Oustaloup. Tutorial on system identification using fractional differentiation models. In *SYSID*, pages 606–611, Newcastle, Australia, 2006.

D.W. Marquardt. An algorithm for least-squares estimation of non-linear parameters. *J. Soc. Industr. Appl. Math.*, 11(2):431–441, 1963.

B Mathieu, A Oustaloup, and F. Levron. Transfer function parameter estimation by interpolation in the frequency domain. In *EEC'95*, Rome, Italie, 1995.

D. Matignon. Stability properties for generalized fractional differential systems. *ESAIM proceedings - Systèmes Différentiels Fractionnaires - Modèles, Méthodes et Applications*, 5, 1998.

K.B. Oldham and J. Spanier. The remplacement of fick's laws by a formulation involving semi-differentiation. *Electro-anal. Chem. Interfacial Electrochem*, 26:331–341, 1970.

K.B. Oldham and J. Spanier. A general solution of the diffusive equation for semiinfinite geometries. *Journal of Mathematical Analysis and Applications*, 39:655–669, 1972.

K.B. Oldham and J. Spanier. Diffusive transport to planar, cylindrical and spherical electrodes. *Electroanaly. Chem. Interfacial Electrochem.*, 41:351–358, 1973.

K.B. Oldham and J. Spanier. *The fractionnal calculus - Theory and Applications of Differentiation and Integration to Arbitrary Order*. Academic Press, New-York and London, 1974.

A. Oustaloup. *La dérivation non-entière*. Hermès - Paris, 1995.

B. Riemann. Gesammelte werke. 1892.

S. Rodrigues, N. Munichandraiah, and A.-K. Shukla. A review of state of charge indication of batteries by means of A.C. impedance measurements. *Journal of Power Sources*, 87:12–20, 2000.

J. Sabatier, M. Aoun, A. Oustaloup, G. Grégoire, F. Ragot, and P. Roy. Fractional system identification for lead acid battery sate charge estimation. *Signal Processing*, 86(10):2645–2657, 2006.

J. Sabatier, M. Merveillaut, R. Malti, and A. Oustaloup. On a representation of fractional order systems: Interests for the initial condition problem. In *3rd IFAC Workshop on Fractional Differentiation and its Applications, FDA'08*, Ankara, Turkey, 2008.

S.G. Samko, A.A. Kilbas, and O.I. Marichev. *Fractional integrals and derivatives: theory and applications*. Gordon and Breach Science, 1993.